Preliminaries on a lattice analysis of the pion light-cone wave function: A partonic signal?

A. Abada, Ph. Boucaud, G. Herdoiza, J. P. Leroy, J. Micheli, and O. Pène
Laboratoire de Physique Théorique, Université de Paris XI, Bâtiment 211, 91405 Orsay Cedex, France

J. Rodríguez-Quintero
Departmento de Física Aplicada e Ingeniería Eléctrica, E.P.S. La Rábida, Universidad de Huelva, 21819 Palos de la fra., Spain
(Received 25 May 2001; published 11 September 2001)

We present the first attempt of a new method to compute the pion light-cone wave function (LCWF) on the lattice. We compute the matrix element between the pion and the vacuum of a nonlocal operator: the propagator of a ''scalar quark'' (named, for short a ''squark''). A theoretical analysis shows that for some kinematical conditions (an energetic pion and hard squark) this matrix element depends dominantly on the LCWF $\Phi_\pi(u), u \in [0,1]$. On the lattice, the discretization of the parton momenta imposes further constraints on the pion momentum. The two-point Green functions made of squark-quark and squark-squark fields show a hadronlike bound-state behavior and verify the standard energy spectrum. We show some indications that during a short time, after being created, the system of the spectator quark and the squark behave like partons, before they form a hadronlike bound state. This short time is the place where the partonic wave function has to be looked for.

DOI: 10.1103/PhysRevD.64.074511 PACS number(s): 11.15.Ha, 11.10.St, 12.38.Gc, 13.20.Cz

I. INTRODUCTION

The light-cone wave functions[1] (LCWF's) [1] enter the calculation of a large variety of processes such as electroweak decays, diffractive processes, meson production in e^+e^- and $\gamma\gamma$ annihilation, relativistic heavy ion collisions, heavy flavors, and many others [2].

The LCWF depends on a large momentum scale μ^2, which is typically the momentum of the considered hadron P_z^2 in a physically well chosen reference frame (e.g., equal velocity frame for form factors, B rest frame for B decay, etc.). The pion wave function is expanded in terms of Fock states:

$$|\pi\rangle = a_1|q\overline{q}\rangle + a_2|q\overline{q}g\rangle + a_3|q\overline{q}gg\rangle + \cdots, \qquad (1)$$

where the lowest Fock state $|q\overline{q}\rangle$ describes the valence configuration which is dominant at large enough P_z^2 [3]. Up to power corrections $O(\Lambda_{\rm QCD}^2/P_z^2)$, the valence component $|q\overline{q}\rangle$ is fully described by its leading twist amplitude.

The leading twist amplitude has been proven to be describable in a very compact and frame independent way: the wave function $\Phi_\pi(u)$ is defined by the following matrix element involving the π^- meson and a light cone Wilson string:

$$\langle 0|\overline{d}(0)\mathcal{P}\left[\exp\left(i\int_x^0 d\tau_\mu A^\mu\right)\right]\gamma_\mu\gamma_5 u(x)|\pi^-(p)\rangle_{x^2=0} = -ip_\mu f_\pi \int_0^1 du\, e^{-iup\cdot x}\Phi_\pi(u). \qquad (2)$$

The Wilson string in the square brackets ensures the gauge invariance of the left-hand side (LHS) of Eq. (2). The link between the first term in Eq. (1) and $\Phi_\pi(u)$ will be discussed in Sec. II A.

Let us notice here that Eq. (2) describes the LCWF a la Bethe-Salpeter (BS), but, although the Bethe-Salpeter framework differs significantly from the null-plane quantization approach, Eq. (2) exactly describes the dominant contribution to the pion wave function on a null plane. It is also useful to remember that the null-plane quantized wave function on a plane $t+z=0$, is equal to the pion wave function quantized on $t=$constant, for a pion with a momentum $P_z=\infty$. In Eq. (2) u denotes the longitudinal momentum fraction of the pion carried by the (valence) quark in the infinite momentum frame. The antiquark carries a fraction $(1-u)$.

Let us insist, the pion wave function in QCD is an extremely complicated object, which cannot be reduced to the BS wave function on the light cone.[2] However, in its infinite momentum frame, it simplifies dramatically in the following sense: the form factors depend only on the longitudinal wave function defined in Eq. (2) while the transverse motion of quarks becomes irrelevant. For finite but large pion momenta the corrections are $O(\Lambda_{\rm QCD}^2/P_z^2)$. Equivalently, for a quark and an antiquark lying almost on the same light line a corrective term $O(x^2\Lambda_{\rm QCD}^2)$ has to be added to the LHS of Eq. (2) if this is not to be restricted to $x^2=0$.

Systematic expansions in inverse powers $\Lambda_{\rm QCD}^2/P_z^2$ may be performed. But, even better, for each order in $\Lambda_{\rm QCD}^2/P_z^2$, perturbative QCD (pQCD) methods [1,4,5] allow the coefficients to be systematically expanded in powers of $1/\log(P_z^2/\Lambda_{\rm QCD}^2)$.

The dominant term in this perturbative expansion, i.e., the asymptotic form of the LCWF for very large $\mu^2 \sim P_z^2$ reads:

[1]We use the expression ''light cone'' wave function according to a common habit, although a ''null plane'' wave function is more appropriate since the quantification surface is indeed a null plane.

[2]The light cone is a surface of zero measure in full space time.

$$\Phi_\pi^{\rm as}(u) = 6u(1-u). \tag{3}$$

In this extreme limit, the shape of the wave function is totally given by pQCD, while the multiplicative constant f_π in Eq. (2) contains all the relevant nonperturbative knowledge. The function Eq. (3) is corrected by terms that decrease only logarithmically when $\mu^2 \to \infty$. While the anomalous dimensions of these terms are computable from pQCD, their coefficients are only computable by nonperturbative methods or to be taken from experiment.

At lower μ^2, when the $O(\Lambda^2_{\rm QCD}/\mu^2)$ power corrections can still be neglected but not the logarithmic $O(1/\log(\mu^2/\Lambda^2_{\rm QCD}))$ ones, the form of the wave function evolves away from Eq. (3). The study of the LCWF in this range needs the use of nonperturbative methods. Most frequently one computes the LCWF via moments of the function $\Phi_\pi(u)$ as will be shortly described in the next paragraph. A well known example is the work by Chernyak and Zhitnitsky (CZ) [6] who used the QCD sum rules[3] to determine the first two moments and determined that at $\mu = 1$ GeV the shape of the pion wave function is completely different from its asymptotic form and it is written:

$$\Phi_\pi^{\rm CZ}(u) = 120u(1-u)(u-0.5)^2. \tag{4}$$

As can be seen from Eqs. (3) and (4) there is a large difference between the two functions.

Experimental measurements of the electromagnetic form factors of the pion were considered to be the best way to study these wave functions [8]. Recent model-dependent analyses of CLEO data on meson-photon transition form factors [9,10] are consistent with the asymptotic wave function. A direct measurement [11] was carried out using data on diffractive dissociation of 500 GeV/c π^- into di-jets from a platinum target at Fermilab experiment E791. The results show that the asymptotic wave function Eq. (3) describes the data well for $\mu^2 \sim 10$ $({\rm GeV}/c)^2$ or more, although this interpretation is subject to some controversy [12].

On the theoretical side, a direct nonperturbative measurement of the LCWF is badly needed. There are only few attempts in that direction. The first method [13] is a lattice computation of moments of the LCWF

$$\mathcal{M}_n = \int_0^1 du\, u^n \Phi_\pi(u), \tag{5}$$

which can be done by computing the pion to vacuum matrix elements of local operators such as

$$\langle \pi^-(\vec{p}_\pi)|\overline{d}(0)\gamma^\mu\gamma_5(iD^{\mu_1})\ldots(iD^{\mu_n})u(0)|0\rangle = -if_\pi \mathcal{M}_n p_\pi^\mu p_\pi^{\mu_1}\ldots p_\pi^{\mu_n} + \cdots,$$

where the dots at the end correspond to terms suppressed by powers of $\Lambda^2_{\rm QCD}/P_z^2$ [the same terms have been eliminated in the LHS of Eq. (2) by means of the restriction $x^2 = 0$]. The lattice discretization of the derivative operators in Eq. (6) is more and more tricky with higher moments, and their renormalization is not easy either.

It was therefore proposed in [14] that we attempt a direct calculation of the LCWF from lattice QCD. One tries to ''see'' on the lattice *the partonic constituents* of the hadrons instead of the hadrons themselves. The idea is first to consider an energetic pion, which is supposed to have its partonic constituents ''frozen'' by Lorentz boost, and second to hit one of its quarks by giving it a large momentum in order to measure the perturbative part (small distance between the constituents) of the wave function. Having scalar with the color content of quarks propagating from the hit quark to the spectator ensures gauge invariance.

In this paper we report the first and preliminary real attempt in that direction. In Sec. II we explain the principle of the calculation and derive the basic formulas, taking care to establish which parameters of the run we may expect the subdominant contributions to the pion wave function to be under control. In Sec. III we describe the lattice setup used. In Sec. IV we present the results on the two-point Green functions. In Sec. V we present the results on the three-point Green function and present the main analysis of our result. We believe that our results might provide some hint of a partonic behavior. Finally, we discuss the relevance of our results in Sec. VI.

II. PRINCIPLE OF THE CALCULATION

In this section we want to elaborate on some theoretical tools necessary to prepare the direct lattice calculation of the LCWF. The issue is to reach some understanding of what to run on a lattice to measure the pion LCWF and to estimate the expected uncertainties. On a lattice, it is clearly impossible to directly measure the matrix element in Eq. (2) since it is obvious that the Euclidean metric has no light cone. The large momentum frame approach is more promising, with a standard continuation to imaginary time. We will then need to take into consideration the full pion wave function, assuming from QCD some general knowledge about it, and then consider under which conditions what is measured in the lattice depends dominantly on the LCWF, and if so, to estimate the subleading contributions. This will first be performed in Lorentz metric in an infinite volume. Later on we will take into account the Euclidean metric and the finite volume effects.

A. Derivation of the basic formulas

From now on, we will use the Light-cone gauge, where the path ordered operator $\mathcal{P}\exp(i\int_x^0 d\tau_\mu A^\mu)$ is equal to 1. Equation (2) defines the pion Bethe and Salpeter wave function on the light cone, which has been extensively studied in literature since the pioneering work of Brodski and Lepage [1]. It contains the leading contribution to the pion wave function, the subleading pieces having been eliminated by

[3]These QCD sum rules for the first two moments of the pion twist-two distribution amplitude were recalculated in Ref. [7] resulting in a shape between the two extreme cases $\Phi^{\rm as}$ and $\Phi^{\rm CZ}$.

the light cone condition $x^2=0$. We are aiming at a lattice investigation of this wave function. This will lead us (as already done in Ref. [14]) to compute Fourier integrals of the wave function over the whole space and not only on the light cone. Therefore, the effect of subdominant contributions should be considered. Luckily, hadron properties, as derived from QCD asymptotic freedom, allow us to control the approximation introduced when neglecting these subdominant contributions.

Let us follow the standard light-cone perturbation theory (LCPth) techniques [1]. We consider the first term in Eq. (1), i.e., the valence $\bar{u}-d$ Fock state[4] for the π^- meson wave function resulting from the quantification on the null-plane time, i.e., $x^+=t+z=0$ $(V^{+(-)}=V_0+(-)V_z)$:

$$\begin{aligned}\langle 0|\bar{d}(0)\gamma^+\gamma_5 u(\underline{x})|\pi(\underline{p})\rangle_{x^+=0}&\\ =-ip^+f_\pi\int_0^1 du\, e^{-iu(p^+x^-)/2}\int\frac{d^2\vec{k}_\perp}{(2\pi)^2}&\\ \times e^{i\vec{k}_\perp\cdot\vec{x}_\perp}\psi^-_{\bar{u}d/\pi}(u,\vec{k}_\perp)&\\ =-ip^+f_\pi\int_0^1 du\, e^{-iu(p^+x^-)/2}\tilde{\psi}^-_{\bar{u}d/\pi}(u,\vec{x}_\perp),&\end{aligned} \tag{6}$$

where the change of variable $k^+=up^+$ has been performed, with $0\leqslant u\leqslant 1$ since both the "+" components of quark (up^+) and antiquark $[(1-u)p^+]$ have to be positive (remember that components "+" of momenta have to be positive by definition) and where $\tilde{\psi}^-_{\bar{u}d/\pi}(u,\vec{x}_\perp)$ is the partial Fourier transform (over $\vec{k}_\perp$) of $\psi^-_{\bar{u}d/\pi}(u,\vec{k}_\perp)$.

The previous matrix element depends on the light-cone three-momentum $\underline{p}=(p^+,\vec{p}_\perp)$ and its conjugated three vector in configuration space, $\underline{x}=(x^-,\vec{x}_\perp)$. For the sake of simplicity, we chose the frame where $\vec{p}_\perp=0$, and hence $p\cdot x \equiv p^+x^-/2$. The wave function $\psi^-_{\bar{u}d/\pi}(u,\vec{k}_\perp)$ in Eq. (6) represents the probability amplitude for finding two partons with momenta $(up^+,\vec{k}_\perp)$ and $(p^+(1-u),-\vec{k}_\perp)$, respectively, in the valence Fock state of the pion. This amplitude is normalized to 1,

$$\int_0^1 du\int\frac{d^2\vec{k}_\perp}{(2\pi)^2}\psi^-_{\bar{u}d/\pi}(u,\vec{k}_\perp)=\int du\,\tilde{\psi}^-_{\bar{u}d/\pi}(u,0)=1, \tag{7}$$

as it immediately comes from requiring that $\langle 0|\bar{d}\gamma^+\gamma_5 u|\pi\rangle=-ip^+f_\pi$ when the operator becomes local, i.e., when $\underline{x}=0$ in Eq. (6).

In Eq. (6) we have only considered the γ_μ component in the direction "+" of the pion momentum. The other directions $\gamma^\perp$ and γ^- can lead to matrix elements proportional, respectively, to $p^\perp$ and p^-. In the pion rest frame all these components of the matrix elements should be of order $\Lambda^2_{\rm QCD}$ if we do not assume any restriction[5] on x. This simply expresses that the size of the pion in its rest frame is $O(\Lambda_{\rm QCD})$ in momentum space and $O(1/\Lambda_{\rm QCD})$ in configuration space. Let us now consider a frame in which the pion has a very large p^+. Then the matrix element considered in Eq. (6) is increased proportionally to the increase of p^+; however, on the contrary x^- is decreased by the same ratio and the transverse components remain constant. For an "infinite momentum" pion we are left only with the contribution proportional to the pion momentum. This is a first indication that in our analysis we will have to concentrate on energetic pions.

Equation (6) is a definition of the wave function $\psi^-_{\bar{u}d/\pi}(u,\vec{k}_\perp)$. It only depends on the quantities u (the fraction of pion's momentum carried longitudinally by one parton) and $\vec{k}_\perp$; it is frame independent for longitudinal boosts. In order to establish the connection with Eq. (2), we now put $x^2=0$ (i.e., $\vec{x}_\perp=0$ provided that we quantized on the light-cone time $x^+=0$) in Eq. (6). If we take $\vec{x}_\perp=0$ in Eq. (6) and compare the result with Eq. (2) we see that[6]

$$\Phi_\pi(u)\equiv\int\frac{d^2\vec{k}_\perp}{(2\pi)^2}\psi^-_{\bar{u}d/\pi}(u,\vec{k}_\perp)=\tilde{\psi}^-_{\bar{u}d/\pi}(u,0). \tag{8}$$

To clarify the physical picture let us now compare in the Light-cone gauge the LHS of Eq. (2) unrestricted to $x^2=0$ (the full BS equation) and the LHS of Eq. (6). They only differ by the null plan constraint $x^+=0$. This constraint is generated by requiring that the pion carry a large momentum. Indeed $p^-=m_\pi^2/(p_z+E_\pi)$ appears to be powerfully suppressed. This suppression of p^- implies that $p^+x_-+p^-x_+ \simeq p^+x_-$ (unless x^+ is unnaturally large). If one assumes the absence of sudden changes when x^+ moves away from 0, one may replace p^+x_- by px in Eq. (6) which now reads

$$\begin{aligned}\langle 0|\bar{d}(0)\gamma_\mu\gamma_5 u(x)|\pi^-(p)\rangle&\\ =-ip_\mu f_\pi\int_0^1 du\, e^{-iup\cdot x}\tilde{\psi}^-_{\bar{u}d/\pi}(u,\vec{x}_\perp).&\end{aligned} \tag{9}$$

If we add the physical input that the wave function extends typically to transverse momenta on the order of $\Lambda_{\rm QCD}$, we get from $0\leqslant u\leqslant 1$ the picture that the valence constituents of the pion move essentially in the same direction as the pion itself at a velocity close to 1. In other words, due to asymptotic freedom, the constituents do not like to have a very large virtuality and the only way for almost massless

[4]Strictly speaking, we retain only the dominant part of the valence Fock state, the one connected to vacuum via the axial current, the other contributions being suppressed. This suppression can be understood simply from the fact that the quarks in an energetic pion have dominantly the same helicity.

[5]Let us repeat that we are not allowed to restrict ourselves to small x_μ since we will perform Fourier transforms.

[6]Remember that the exponential in brackets in Eq. (2) is equal to 1 in our gauge.

quarks to build up the energy and momentum of the almost massless pion is to move in the same direction, i.e., to have $E_q+E_{\bar{q}} \simeq |k_q|+|k_{\bar{q}}| \simeq E_\pi \simeq |k_q+k_{\bar{q}}|$.

From now on we shall follow the method in [14] and we will replace the gauge invariance restoring operator $\mathcal{P}\exp(i\int_x^0 d\tau_\mu A^\mu)$ by another one, which is easier to continue analytically to euclidean time: the scalar colored propagator

$$S(0;x)=\frac{1}{-\mathcal{D}^2-m_S^2+i\epsilon}\simeq\frac{1}{-\partial^2-m_S^2+i\epsilon}$$

$$=\int\frac{d^4k}{(2\pi)^4}e^{-ik\cdot(0-x)}\frac{i}{k^2-m_S^2+i\epsilon}, \qquad (10)$$

where m_S is a mass parameter, assumed to be small or zero to mimic a massless parton. In Eq. (10), when replacing $\mathcal{D}^2$ by ∂^2 we have bluntly neglected the coupling to gluons. This has been done in order to simplify the argument which will follow and is justified if we assume the scalar object to be ''hard'' and hence to behave mainly as a parton. Still, a careful study of the effect of radiative corrections is strongly needed. This replacement loses the gauge invariance of the $1/\mathcal{D}^2$ operator. This is difficult to avoid: if the light cone wave function Eq. (2) is gauge invariant, the more general ones, Eq. (9), are not. Here the loss of gauge invariance is the price we pay to present the argument that will follow. Needless to say, the real lattice calculations have been performed in a gauge invariant way.

We can thus write

$$e^{-iq\cdot x}\langle 0|\bar{d}(0)\gamma_\mu\gamma_5 S(0;x)u(x)|\pi(p)\rangle$$

$$=-ip_\mu f_\pi\int_0^1 du\int\frac{d^4k}{(2\pi)^4}e^{-i(up+q-k)\cdot x}$$

$$\times\frac{i}{k^2-m_S^2+i\epsilon}\tilde{\psi}_{\bar{u}d/\pi}(u,\vec{x}_\perp). \qquad (11)$$

This is supposed to be valid for all x so that we can integrate over $\vec{x}$ and obtain

$$i\int d^3x e^{-iq\cdot x}\langle 0|\bar{d}(0)\gamma_\mu\gamma_5 S(0;x)u(x)|\pi(p)\rangle = p_\mu f_\pi\int_0^1 du\int\frac{dk_0}{2\pi}dk_z\frac{d^2\vec{k}_\perp}{(2\pi)^2}e^{i(uE_\pi-k_0)t}\frac{i\delta(up_z+q_z-k_z)}{\vec{k}_{//}^2-\vec{k}_\perp^2-m_S^2+i\epsilon}\psi_{\bar{u}d/\pi}(u,\vec{q}_\perp-\vec{k}_\perp)$$

$$=-p_\mu f_\pi\int_0^1 du\int\frac{d^2\vec{k}_\perp}{(2\pi)^2}\frac{e^{i(uE_\pi-\sqrt{(up_z+q_z)^2+(\vec{q}_\perp+\vec{k}_\perp)^2+m_S^2})t}}{2\sqrt{(up_z+q_z)^2+(\vec{q}_\perp+\vec{k}_\perp)^2+m_S^2}}\psi_{\bar{u}d/\pi}(u,-\vec{k}_\perp) \qquad (12)$$

where $q_0=0$, $x_0=-t$ $(t<0)$, $\vec{k}_{//}=(k_0,k_z)$, and again $\vec{p}_\perp=0$. The right-hand side of the latter line derives from integrating the former's over $\vec{k}_{//}$ and changing variables $(q-k)_\perp\to-k_\perp$.

At this stage let us return to the physical understanding of the wave function $\psi_{\bar{u}d/\pi}(u,-\vec{k}_\perp)$ already briefly considered above. The quarks have a small probability of being far off shell and $\psi_{\bar{u}d/\pi}(u,\vec{k}_\perp)$ vanishes when $\vec{k}_\perp^2$ becomes large.[7] In practice, $\vec{k}_\perp^2\psi_{\bar{u}d/\pi}(u,\vec{k}_\perp)\to 0$ as $\vec{k}_\perp^2\to\infty$ [1]. Therefore, this suppression for large $\vec{k}_\perp^2$ allows one to expand in powers of the transverse components, provided that $E_S\gg\Lambda_{\rm QCD}$; $\Lambda_{\rm QCD}$ being a natural hadronic energy scale *bounding* the transverse momentum carried by the partons and

$$E_S\equiv\sqrt{(up_z+q_z)^2+q_\perp^2+m_S^2}. \qquad (13)$$

We then get

$$i\int d^3x e^{-iq\cdot x}\langle 0|\bar{d}(0)\gamma_\mu\gamma_5 S(0;x)u(x)|\pi(p)\rangle$$

$$=-p_\mu f_\pi\int_0^1 du\frac{e^{i(uE_\pi-E_S)t}}{2E_S}\Bigg[\Phi_\pi(u)+\int\frac{d^2\vec{k}_\perp}{(2\pi)^2}$$

$$\times\left\{e^{-i[(2\vec{k}_\perp\cdot\vec{q}_\perp+\vec{k}_\perp^2)/2E_S]t}\left(1-\frac{2\vec{k}_\perp\cdot\vec{q}_\perp+\vec{k}_\perp^2}{2E_S^2}\right)-1\right\}$$

$$\times\psi_{\bar{u}d/\pi}(u,-\vec{k}_\perp)\Bigg]+\cdots, \qquad (14)$$

It is easy to see that the second term inside the bracket (last line) is formally $O(\Lambda_{\rm QCD}/E_S)$, provided that $t\ll E_S/\Lambda_{\rm QCD}^2$ and $t\ll E_S/(\Lambda_{\rm QCD}|\vec{q}_\perp|)$. This second term is negligible as long as, and this is the general situation, $E_S\sim[|up_z+q_z|^2$

[7] Perturbative analysis indicates that hadronic wave functions do not decrease quickly enough as $\vec{k}_\perp^2\to\infty$ to avoid the appearance of infinities. The pion $\bar{q}q$ wave function falls off roughly as $1/\vec{k}_\perp^2$ [1], and the resulting ultraviolet logarithmic divergence is the origin of the scale dependence of the wave function. For the sake of simplicity this point shall be deliberately overlooked in our formal derivation.

$+q_\perp^2]^{1/2} \gg \Lambda_{\rm QCD}$.[8] However, when $|up_z+q_z| \sim \Lambda_{\rm QCD}$ for some values of u and when $q_\perp \lesssim \Lambda_{\rm QCD}$, i.e., when $\vec{p}$ and $\vec{q}$ are back to back,[9] the expansion in Eq. (14) breaks down as E_S is not larger than $\Lambda_{\rm QCD}$ any longer. In other words, giving a large transverse kick to the pion generates a hard gluon exchange between quarks, which selects the perturbative component of the pion wave function, the so-called ''small pion,'' which is what we want to measure. Indeed in the Fermilab experiment E791 [11], the LCWF is observed via jets which have rather large transverse momenta. Let us now summarize.

Conditions for a partonic signal [C1]

In order to determine on the light-cone wave function $\Phi_\pi(u)$ from the lattice calculation of the LHS of Eq. (14), the following conditions are required beyond the general large pion momentum constraint, i.e., $p_z \gg \Lambda_{\rm QCD}$: $t \ll E_S/\Lambda_{\rm QCD}^2$, $t \ll E_S/(\Lambda_{\rm QCD}|\vec{q}_\perp|)$, and $E_S \gg \Lambda_{\rm QCD}$ for all u. This generally implies $\cos_{\rm min} \lesssim \cos\theta_{pq}$ for some $\cos_{\rm min}$ significantly greater than -1.

B. Consequences of discrete partonic momenta

Let us now consider a finite parallelepipedic volume with periodic boundary conditions (torus). As is well known, the momenta components can only take the form

$$p_\mu = \frac{2\pi}{L_\mu} n_\mu, \tag{15}$$

where n_μ are integers and L_μ is the length in the direction μ. This is obviously also valid for partonic momenta.[10] Thus in the formulas of Sec. II A all integrals over $\int_0^1 du$ have to be replaced by discrete sums over the values of u such that up_μ verifies Eq. (15).

There is an immediate problem. Let us assume for one moment that the components of p_μ are all 0 or $2\pi/L_\mu$. Then only the values $u=0,1$ are allowed. In any model the LCWF which is proportional to $u(1-u)$, Eqs. (3) and (4), vanish for these values. The expected dominant behavior at large momentum vanishes in this case, and only subdominant effects can be observed.

The simplest situation, the only one considered from now on, is when the pion momenta are aligned along one of the lattice spatial directions μ. To allow values of u that scan the domain of variation $[0,1]$ densely[11] enough to provide a fair description of the LCWF we should have

$$p_\mu \gg \frac{2\pi}{L_\mu}. \tag{16}$$

This condition [C2] has to be added to the set of conditions [C1] summarized at the end of Sec. II A in the case of infinite volume. Clearly this new one *is not* equivalent to the former ones since this one does depend on L_μ and disappears smoothly in the large volume limit.

C. Strategy for lattice calculations

Following the method of [14] on the lattice we compute the three-point Green function

$$F^\mu(\vec{p},\vec{q};t) \equiv \int d^3y\, d^3x\, e^{-i\vec{q}\cdot\vec{x}} e^{-i\vec{p}\cdot\vec{y}} \langle 0|P_5(\vec{y},t_\pi) u(\vec{x},t) \times S(\vec{x},t;0)\gamma_\mu\gamma_5 \overline{d}(0)|0\rangle e^{E_\pi(t_\pi - t)}. \tag{17}$$

When all the conditions [C1] and [C2] are satisfied, and after performing a Wick rotation to Euclidean metric, the LHS of Eq. (17) approximately verifies the following proportionality in terms of the LCWF:

$$F^\mu(\vec{p},\vec{q};t) \propto p_\mu f_\pi \sum_{u_i} \frac{e^{-((1-u_i)E_\pi + E_S)t}}{2E_S(u_i)} \Phi_\pi(u_i), \tag{18}$$

where the Σ_i extends over all values $0 \leqslant u_i \leqslant 1$ such that $u_i p_\mu * L/(2\pi)$ are integers. $\vec{p}$ is the momentum of the pion generated by the interpolating field $P_5(y) \equiv \overline{d}(y)\gamma_5 u(y)$, and $\vec{q}$ is a momentum given to one valence quark of the pion. $E_S(u)$ is defined in Eq. (13). We have assumed $0 < t < t_\pi$. The $e^{E_\pi(t_\pi - t)}$ takes into account the propagation of the pion between t and t_π. Of course $t_\pi - t$ has been assumed to be large enough to eliminate the excited pseudoscalar states.

Equation (18) may be understood in a simple way: the time evolution between 0 and t is the product of the propagators of two ''partons,'' one scalar parton of energy E_S with a propagator proportional to $e^{-E_S t}/(2E_S)$ and the spectator quark of energy $(1-u)E_\pi$. The scalar parton has the color quantum numbers of a quark. For convenience let us call it a squark, although it has obviously nothing to do with supersymmetry. The three-point Green function in Eq. (17) could also be used to estimate the form factor for the transition between a pion and squark-quark bound state (which we call a pionino, $\tilde{\pi}$, to follow on the same metaphoric nomenclature). In such a case we would take t large enough for the ground state pionino to dominate:

$$F^\mu(\vec{p},\vec{q};t) \underset{t\to\infty}{\propto} e^{-E_{\tilde{\pi}} t}, \tag{19}$$

where $E_{\tilde{\pi}}$ is the pionino energy. For small t, on the contrary, the excited states should add up coherently in a complicated manner. The analysis presented in Sec. II D seems to indicate that this should boil down to a rather simple partoniclike picture. In other words we expect a kind of hadron-parton duality to be at work for small t which should allow a partonic reading of our data. At this stage it is clear that we need

---

[8] Remember that m_S is small.

[9] Strictly speaking $\vec{p}$ and $\vec{q}$ could be back to back as long as $|q_z| - |p_z| \gg \Lambda_{\rm QCD}$.

[10] For other values the amplitudes are canceled by destructive interferences.

[11] The dominant contribution to the LCWF is only possible when all the $n_\mu, \mu = 1,3$ are 0 or have a common divisor, and at least one n_μ is larger than 1.

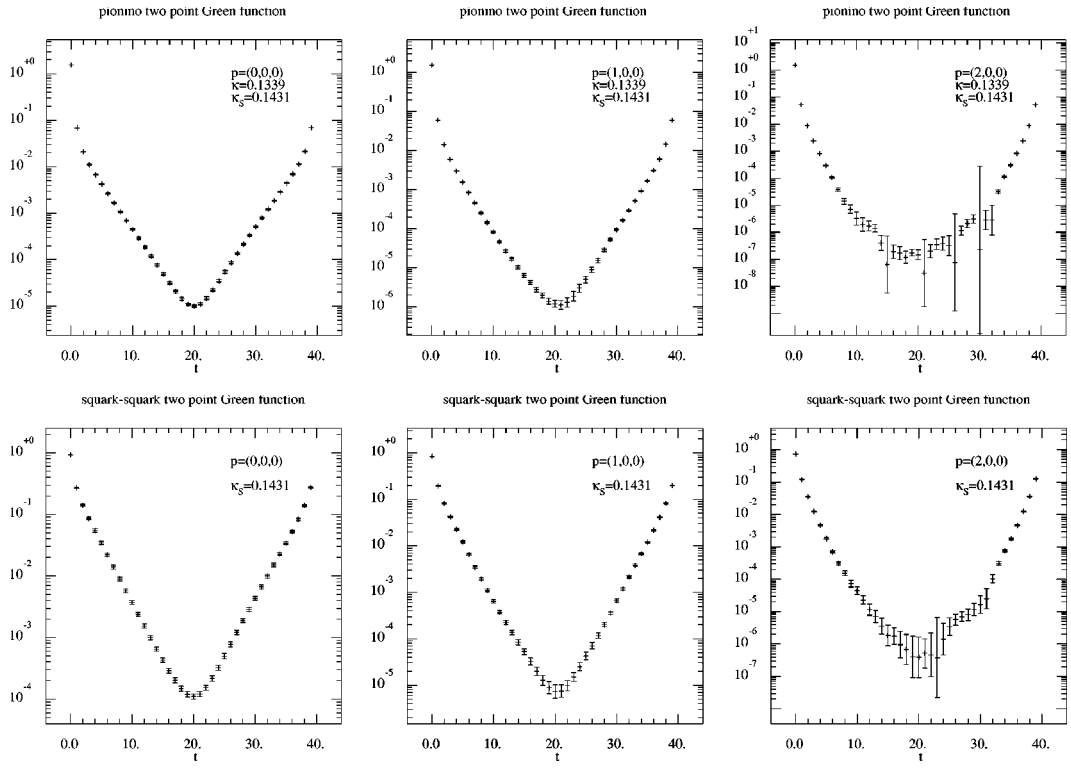

FIG. 1. Two point Green functions in logarithmic plots for pionino and squark-squark states. As an example we present the lightest states, i.e., $\kappa=0.1339$ and $\kappa_S=0.1431$.

to study, beyond the three-point function in the LHS of Eq. (17), the two-point function corresponding to the pionino interpolating field.

An additional comment concerns the squark mass. In the preceding formulas we have written a squark mass m_S as a free parameter. In order to gain the richest possible information on the pion wave function, the renormalized squark mass has to be as light as possible. How do we perform this? We have chosen an approach based on an analogy with QCD hadrons. We will vary the bare squark mass down to when the algorithm to compute the squark propagator stops converging, which we take as an indication of possible zero modes.

Finally, all things considered, we will have to make a systematic study of the spectrum of all the colorless bound states constituted by quarks and squarks. It will turn out that in the quenched approximation nice exponential behaviors do indeed appear, signaling the existence of pioninos and squark-squark bound states (see Fig. 1), and furthermore, for nonvanishing momenta, they follow the relativistic spectral law $E=\sqrt{m^2+p^2}$ (see Fig. 2), or if one prefers the lattice one [see Eq. 22) below], which is not distinguishable from the former within our statistical errors.

D. Symmetries

Before turning to the actual calculation, it is useful to summarize which among the two- and three-point Green functions we intend to compute should vanish because of QCD's discrete symmetries.

In general all Green functions we consider are real in configuration space. Therefore they are real in momentum space if parity-even and imaginary if parity-odd. See Table I.

III. LATTICE SETUP

We consider a $16^3\times 40$ lattice at $\beta=6.0$ in the quenched approximation. The quarks are computed with the clover action with the coefficient $c_{\rm sw}=1.769$. We have used for the spectator quark two values of the bare mass parameters: $\kappa=0.1333$ and 0.1339, and for the active one $\kappa=0.1339$.

The squark propagator $D(x,0)$ verifies the equation

$$\left[\delta_{x,y}-\kappa_S\sum_\mu\ (U_\mu(x)\,\delta_{x,y-\hat{\mu}}+U_\mu^\dagger(x-\hat{\mu})\,\delta_{x,y+\hat{\mu}})\right]D(y,0)=\delta_{x,0}\,. \tag{20}$$

We compute the squark propagator with the bare mass parameter $\kappa_S=$ 0.1428, 0.1430, and 0.1431. Above $\kappa_S=0.1431$ the convergence of the inverter becomes very long, which we take as a sign that we are close to the massless squark.

In each case we have run 100 configurations. The errors are computed according to the jackknife method. The pion interpolating field P_5 is inserted at $t_\pi=16$. This has been chosen so that the direct signal at small t is not significantly perturbed by the signal which has looped around via the end of the lattice: 40–16 has eight time intervals more than 16. This is an important precaution. Indeed from Table I we learn

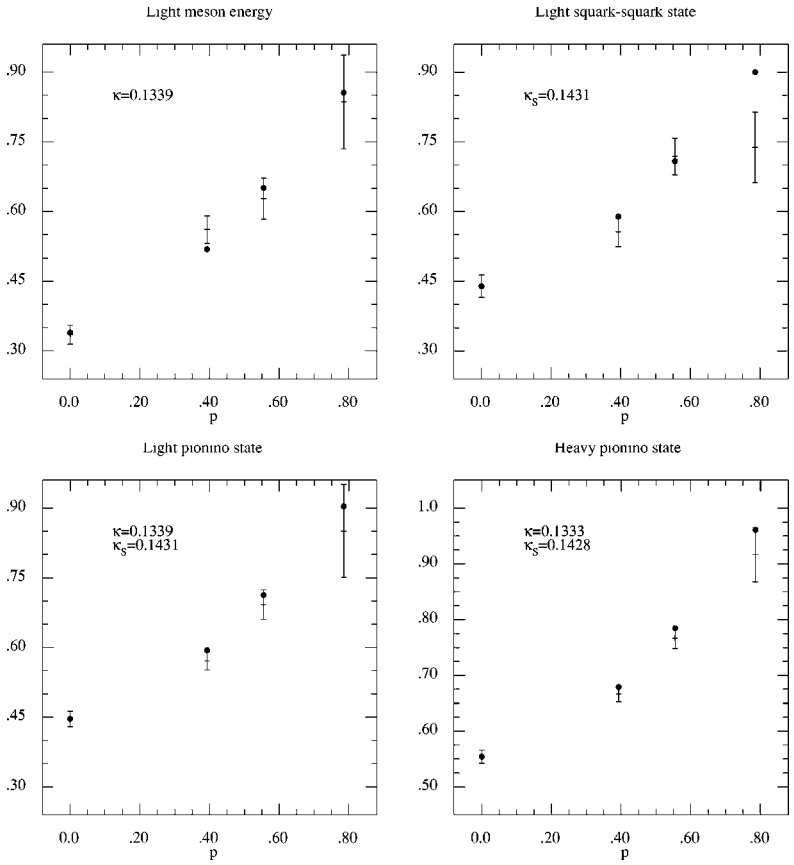

FIG. 2. Energy of the bound states as a function of the momentum in lattice units. The dots correspond to the continuum formula $E=\sqrt{m^2+p^2}$, the mass being taken as the central value of the zero momentum energy. Three first plots are with $\kappa=0.1339, \kappa_S=0.1431$, the last one with $\kappa=0.1333, \kappa_S=0.1428$.

that the three-point Green function with $\gamma_0\gamma_5$ inserted at $t=0$ is odd for time reversal. If t_π was taken in the middle of the lattice, $t=20$, it would have resulted in a vanishing of this three-point Green function for $t=0$. Since we are interested in small values of t such a vanishing of the signal would have made the analysis impossible.

TABLE I. The symmetry properties of the Green functions. By three point we mean the Green function $F^\mu(\vec{p},\vec{q})$ defined in Eq. (17). The second column refers to the γ matrices in the Green function. For squark-quark, only one γ matrix is traced with the quark propagator. In the other cases we indicate the matrices on both ends of the quark propagators. The third column refers to the spatial parity of the Green function. The time reversal refers to the symmetry when $t\to -t$ (and $t_\pi \to -t_\pi$ in the three point case). We thus learn, for example, that the three point with $\gamma_0\gamma_5-\gamma_5$ vanishes at $t=0$ if $t_\pi=t_{\max}/2$.

Operator	γ matrices	Parity	Real/Im	Time reversal	Vanishes at $\vec{p}=0$
Squark-squark	1	+	Real	+	No
Squark-quark	1	+	Real	+	No
Squark-quark	γ_0	+	Real	-	No
Squark-quark	γ_i	-	Imag	+	Yes
Quark-quark	$\gamma_5-\gamma_5$	+	Real	+	No
Quark-quark	$\gamma_0\gamma_5-\gamma_5$	+	Real	-	No
Quark-quark	$\gamma_i\gamma_5-\gamma_5$	-	Imag	+	Yes
Three-point	$\gamma_0\gamma_5-\gamma_5$	+	Real	-	No
Three-point	$\gamma_i\gamma_5-\gamma_5$	-	Imag	+	Yes

For the study of the two- and three-point Green functions we have run with the following values for the pion three momentum:

$$\frac{L\vec{p}}{2\pi}=(0,0,0);(1,0,0);(1,1,0);(2,0,0). \tag{21}$$

In practice, however, the vanishing momentum does not produce a pion describable by a light-cone wave function. The momentum (1,0,0) (1,1,0) will not be useful since in these cases only the values $u=0,1$ are allowed by the discretization and the LCWF vanishes for these values. However, they are kept in the analysis for a comparison of the results obtained from (1,0,0) (1,1,0) with the ones from (2,0,0), which might be interpreted as partonic signal.

Concerning q_μ we have run a large number of momenta, with components ranging from $-(4\pi/L)$ to $(4\pi/L)$ but again too large momenta are too noisy. Later we will detail the momentum configurations considered in the analysis.

As already explained, we hope to catch the partonic signal at small t. In practice we have concentrated on the region $t=0,4$ as we will see later. It leaves $t_\pi - t \geqslant 12$ which should be enough to isolate the pion and it leaves some space to look for plateaus.

IV. TWO-POINT GREEN FUNCTIONS

We have shown in Fig. 1 six examples of new two-point Green functions for momenta $\vec{p}=(0,0,0)$, $\vec{p}=2\pi/L(1,0,0)$, and $\vec{p}=2\pi/L(2,0,0)$, respectively. It is seen that these two-

TABLE II. Energies of the various bound states in units of a^{-1} (for $\beta=6.0, a^{-1}\simeq 2.0$ GeV). The symbols q_1, q_2 represent, respectively, $\kappa=0.1333, 0.1339$ for quarks; $S1, S2, S3$, respectively, $\kappa_S=0.1428, 0.1430, 0.1431$ for scalars. The momentum norms are given in units of $2\pi/L$. We indicate the γ matrices used in the meson interpolating fields.

Momentum	0	1	1.4	2
Pion $q_1 q_1-\gamma_5, \gamma_5$	0.42(2)	0.62(3)	0.70(4)	0.61(13)
Pion $q_1 q_1-\gamma_0\gamma_5, \gamma_0\gamma_5$	0.41(2)	0.60(2)	0.69(3)	0.89(7)
Pion $q_2 q_1-\gamma_5, \gamma_5$	0.38(2)	0.60(3)	0.66(4)	0.35(16)
Pion $q_2 q_2-\gamma_5, \gamma_5$	0.34(2)	0.58(4)	0.61(5)	0.09(22)
Pion $q_2 q_2-\gamma_0\gamma_5, \gamma_0\gamma_5$	0.34(2)	0.56(3)	0.62(4)	0.84(10)
rho $q_1 q_1-\gamma_i, \gamma_i$	0.62(1)	0.76(2)	0.96(3)	1.02(6)
rho $q_2 q_2-\gamma_i, \gamma_i$	0.60(2)	0.71(3)	0.98(5)	0.95(9)
Pionino $q_1 S1-\gamma_0$	0.59(1)	0.71(1)	0.81(1)	0.98(3)
Pionino $q_1 S1-\mathbb{1}$	0.55(1)	0.67(1)	0.77(2)	0.91(5)
Pionino $q_1 S2-\gamma_0$	0.54(1)	0.67(1)	0.77(2)	0.95(3)
Pionino $q_1 S2-\mathbb{1}$	0.51(1)	0.63(2)	0.74(2)	0.88(6)
Pionino $q_1 S3-\gamma_0$	0.51(1)	0.65(2)	0.76(2)	0.93(3)
Pionino $q_1 S3-\mathbb{1}$	0.48(2)	0.60(2)	0.72(2)	0.86(7)
Pionino $q_2 S1-\gamma_0$	0.57(1)	0.70(1)	0.79(1)	0.98(3)
Pionino $q_2 S1-\mathbb{1}$	0.53(1)	0.64(2)	0.74(2)	0.91(7)
Pionino $q_2 S2-\gamma_0$	0.52(1)	0.66(2)	0.76(2)	0.94(3)
Pionino $q_2 S2-\mathbb{1}$	0.48(1)	0.60(2)	0.71(3)	0.87(9)
Pionino $q_2 S3-\gamma_0$	0.49(2)	0.63(2)	0.74(2)	0.92(4)
Pionino $q_2 S3-\mathbb{1}$	0.45(2)	0.57(2)	0.69(3)	0.85(10)
Squark-squark $S1S1$	0.59(2)	0.70(2)	0.80(2)	0.93(5)
Squark-squark $S2S2$	0.50(2)	0.61(2)	0.74(3)	0.83(7)
Squark-squark $S3S3$	0.44(2)	0.56(3)	0.72(4)	0.74(8)

point Green functions do indeed behave as if the quark-squark and squark-squark states were hadronlike bound states.

We present the results for the energies of the bound states in Table II. In Fig 2 we present some checks of the spectral law $E=\sqrt{m^2+p^2}$. The latticized free boson dispersion relation

$$\sinh^2(E/2)=\sinh^2(m/2)+\sum \sin^2(p_\mu/2) \tag{22}$$

does not significantly differ from the continuum one within our errors. For momentum $4\pi/L$ the quark-quark states are in some cases meaningless due to the noise. It is surprising that the nonconventional states present a better signal for this large momentum.

Of course the main lesson of this analysis is that the nonconventional bound states, pioninos, and squark-squark do behave exactly as real hadrons. We are not in a position to discuss the theoretical implications of this fact, nor make any statement about the existence of such bound states in a nonsupersymmetric extension of QCD.

The lowest bare squark mass considered is $\kappa_S=0.1431$. When κ_S is varied slightly above 0.1431, the scalar inverter no longer converges. This squark is coded $S3$ in Table II and we see that the corresponding squark-squark bound state rest mass is about 0.44 in lattice units, i.e., about 900 MeV ($a^{-1}\simeq 2$ GeV for $\beta=6.0$), not far from the rho meson mass. It is rewarding that the mass of this squark-squark bound state is rather light, as if the squark with an approximately vanishing renormalized mass did indeed produce rather light bound states.[12] Indeed we feel encouraged to treat this squark as a light parton as will be done soon.

V. THREE-POINT FUNCTIONS

With our set of momenta, only the momentum $\vec{p}_\pi=2\pi/L$ (2,0,0) gives a nonvanishing[13] $\Phi_\pi(u)$ for discrete $u=1/2$. Thus we will focus our analysis on the latter momentum although we have studied the full set of momenta $\vec{p}_\pi$, with a set of momenta $\vec{q}$ to be discussed later. We have only considered the time component $F^0(\vec{p},\vec{q};t)$.

Our analysis of the data follows from Sec. II C. To test whether Eq. (18) or (19) has some relevance for our data we will consider whether the following quantities

$$F^0(\vec{p},\vec{q};t)\left[p^0 f_\pi \frac{e^{-(E_\pi/2+E_S)t}}{2E_S}\Phi_\pi(1/2)\right]^{-1} \tag{23}$$

and

$$F^0(\vec{p},\vec{q};t)[e^{-E_{\tilde{\pi}}t}]^{-1} \tag{24}$$

are constant in time for some time interval.

Before that, it is instructive to have a look at the numerators $F^0(\vec{p},\vec{q};t)$. As an illustrative example in Fig. 3 we have plotted the three-point function for $\vec{p}_\pi=2\pi/L$ (2,0,0) and various vectors $\vec{q}$. We observe a very striking feature akin to an oscillating behavior. We do not claim to fully understand this shape. However, since in Sec. II a rationale was elaborated to describe the expected partonic behavior which may show up at small time, from now on we will focus on this time interval.

The very rapid drop observed at small time, i.e., $t\in[0,3-4]$ is present for all values of $\vec{q}$. *We will test the hypothesis that this rapid drop is due to a partonic signal* assuming that the hadronic behavior sets in for larger times. The typical shape in Fig. 3 might suggest a negative interference between the small time regime and the latter one, leading to a vanishing amplitude around $t=4$. We do not understand the origin of the latter, which is beyond the scope of this work focused on the small-time drop. It is noticeable that the statistical errors for this time range are small enough to exhibit a signal while the two-point function for the corresponding pion propagation time and the same pion momentum is extremely noisy.

[12]We do not know of any symmetry which would impose a pionlike massless state for massless squarks.

[13]Notice that the CZ wave function (4) vanishes for $u=1/2$, and its study needs even larger momenta and will not be discussed in our analysis.

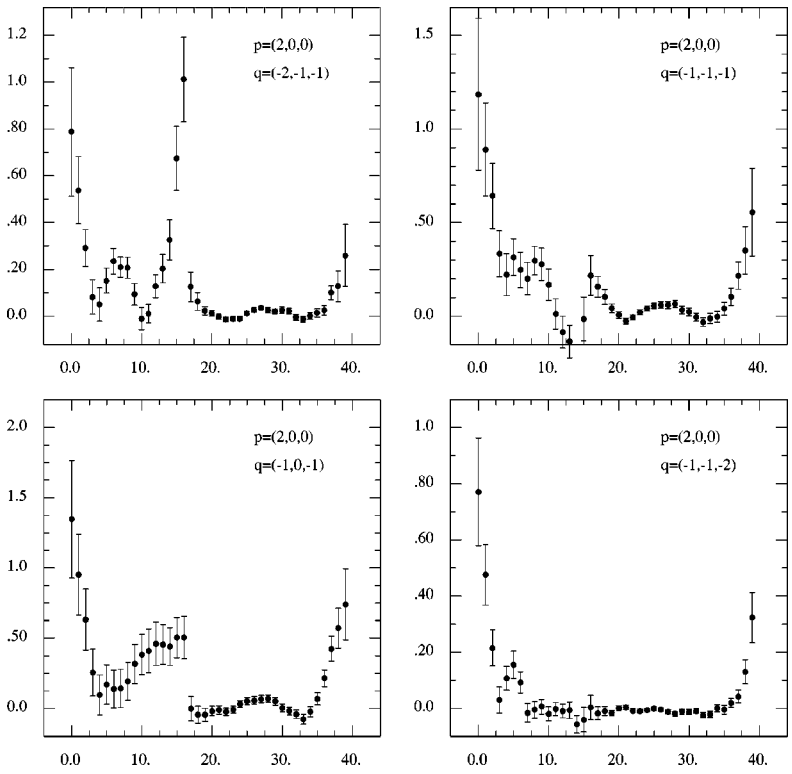

FIG. 3. We plot $F^0(\vec{p},\vec{q};t)$, normalized by a constant [divided by the pion propagator with $\vec{p}=(4\pi/L,0,0)$ from the fixed time t_π to 0] vs the running time for momenta indicated on the plots using the lightest quarks ($\kappa=0.1339$) and the lightest "squark" ($\kappa_S=0.1431$).

A. Searching for plateaus at small times

A plateau of Eq. (23) would indicate a partoniclike behavior, while a plateau of Eq. (24) would indicate a pionino. We will compute E_π and $E_{\tilde{\pi}}$ from the measured pion and pionino rest masses (see Table II), and the formula $E=\sqrt{m^2+p^2}$. We prefer this to the direct use of the measured energies for nonzero momentum, as reported in Table II, because the latter are noisier than the rest masses for $\vec{p}=(2\pi/L)(2,0,0)$.

The energy E_S has been taken via Eq. (13) assuming two possible masses m_S for $\kappa_S=0.1431$. As already mentioned, for $\kappa_S>0.1431$ the calculation of $D(x,0)$ from Eq. (20) fails, indicating the presence of small eigenvalues, i.e., that m_S is small. Besides considering a massless scalar parton ($m_S=0$), we have also considered the value $m_S=0.22$ in lattice units, which corresponds to the scalar-scalar bound state mass (divided by two). It would be tempting to fit m_S from the results, yielding the flattest plateau, but it turned out to be too difficult to disentangle the effect of m_S on the plateau from other effects which will be discussed later.

In Fig. 4 we show two examples of ratios corresponding to Eqs. (23) (left) and (24) (right) at small time. In light of the discussion in Sec. II A, we have chosen to illustrate the following kinematics: $L\vec{q}/(2\pi)=(-2,-1,-1)$ and $L\vec{q}/(2\pi)=(-1,-1,-2)$, both for $L\vec{p}/(2\pi)=(2,0,0)$. It is clearly seen that the plots to the right of Eq. (24) are utterly incompatible with a plateau, thus discarding a pionino interpretation at small time. The plots to the left might show some indication of plateaus but they deserve some discussion. The signal decreases from a maximum at time 0 to reach a value compatible with 0 at a time 3–4. This happens not only for these two examples but is a general pattern for all the kinematics considered. This cancellation has already been seen on the numerators of Eq. (23) in Fig. 3. We have argued that it is motivated by destructive interferences that generate an overdecreasing of the numerators in Eq. (23) with respect to the denominators. The signals vanish as soon as $t=3-4$, restricting the range where plateaus might be seen to a very short time interval[14] around $t=0$.

Anyhow, the most restrictive of the constraints relative to t, summarized at the end of Sec. II A, i.e., $t \ll E_S/(\Lambda_{\rm QCD}|\vec{q}_\perp|)$, amounts, for a massless scalar parton, with our lattice setup and the value $u=1/2$, to the condition

$$t \ll \frac{a^{-1}}{\Lambda_{\rm QCD}} \frac{\sqrt{(p_x/2+q_x)^2+q_\perp^2}}{|q_\perp|} \sim 5, \tag{25}$$

where for $\Lambda_{\rm QCD}$ we have taken a typical quark transverse momentum of 400 MeV within a hadron. This constraint does not allow us to use larger time domains than the one just discussed.

We will now go on confronting the slopes on this small time interval to the theoretical prediction of a plateau for Eq. (23), postponing the maybe more convincing comparative study of the values of $F^0(\vec{p},\vec{q};0)$.

We perform a systematic study over a larger set of three-point Green functions defined such that: $L\vec{p}/2\pi=(2,0,0)$, $(L\vec{q}/2\pi)^2 \leqslant 4$, and $(L(\vec{q}+\vec{p})/2\pi)^2 \leqslant 6$. These limitations on the norm of the momenta are meant to avoid too noisy re-

[14] One may worry about contact terms or other lattice artifacts that might spoil the analysis around $t=0$; this will be discussed in the conclusion.

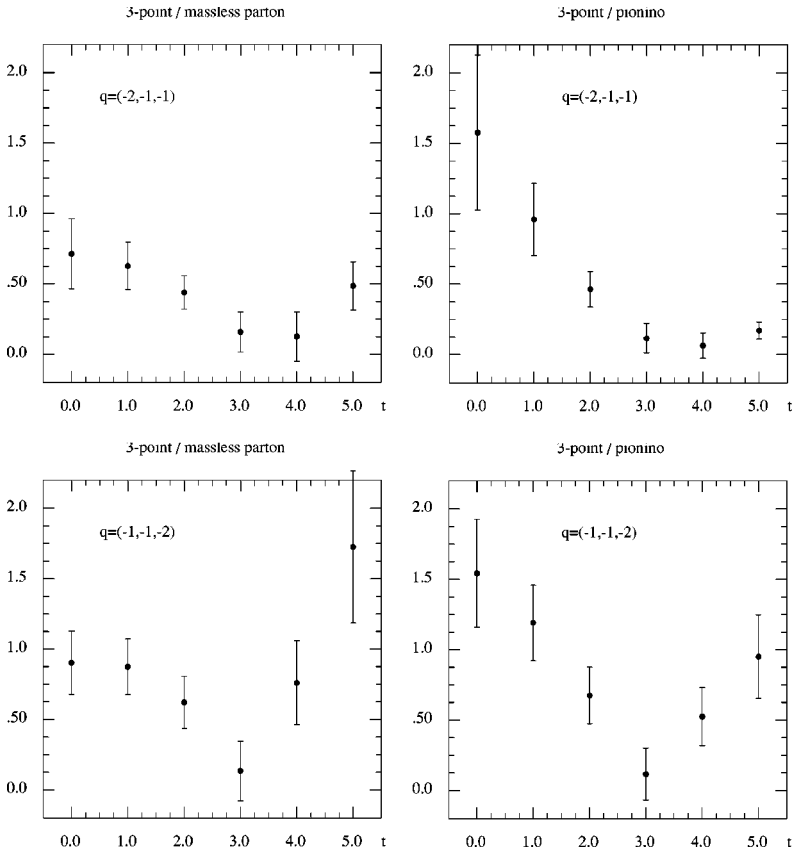

FIG. 4. Ratios of Eqs. (23) (left) and (24) (right) for momenta indicated on the plots using the lightest quarks ($\kappa=0.1339$) and the lightest "squark" ($\kappa_S=0.1431$).

sults. On the other hand, the constraint $E_S \gg \Lambda_{\rm QCD}$ (see Sec. II A) translates into the lower bound:

$$\frac{L}{\pi}\sqrt{\left(\frac{p_x}{2}+q_x\right)^2+q_\perp^2} \gg 1. \tag{26}$$

For this set of data we measure the slope of the ratios in Eqs. (23) and (24) for the time intervals $t=0,3$ and $t=0,4$. For the latter range, the results are presented in Fig. 5: the ratios of Eqs. (23) and (24) are presented for commodity as a function of the cosine of the angle between $\vec{p}$ and $\vec{q}$, which we will from now on be referred to as $\cos\theta_{pq}$.

We have eliminated from the analysis the data with $L\vec{q}/(2\pi)=(-1,0,0)$ for which the scalar parton is at rest $(p_x/2+q_x=0)$ and thus violates the condition Eq. (26). The data with white circles on the plots correspond to $L\vec{q}/(2\pi)=(-1,0,-1)$ which is marginal for both conditions Eqs. (25) and (26). It should be noted that the back-to-back points $L\vec{q}/(2\pi)=(-2,0,0)$ do not raise problems as a result of the discretization of partonic momenta, indeed, since $u=1/2$, $u\vec{p}+\vec{q}$ never vanishes contrarily to the continuum case discussed in Sec. II A. More generally, the majority of the points with $\cos\theta_{pq}$ close to -1 are not excluded for the same reason.

Comparing both plots in Fig. 5, it is evident that the partonic slopes (left) are much closer to zero than the hadronic ones (right). Nevertheless, the partonic slopes show a general tendency to be negative (see Table III) which can be traced back to the vanishing around $t=3-4$. The white circles show

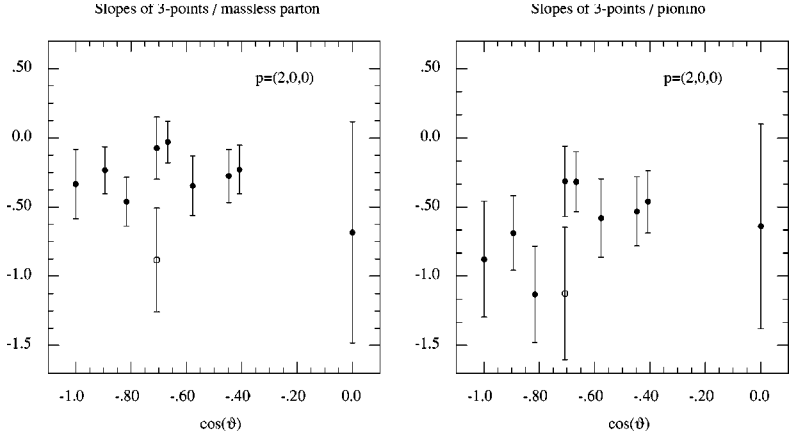

FIG. 5. Slope of the ratios on the time interval t=0,4 for formulas (23) (left) and (24) (right) for different values of $\vec{q}$ and for $\vec{p}=(2\pi/L)(200)$ with a massless scalar parton. The horizontal axis is the cosine of the angle between vectors $\vec{p}$ and $\vec{q}$.

TABLE III. Average slopes (and χ^2/d.o.f for a vanishing slope) of the expression appearing in Eqs. (23) and (24) for two time slices and two parton masses. It is seen that the parton mass does not play a very important role. The difference between the two time slices is due to the zero of F^0 discussed in the text.

Model	Time slice	χ^2/d.o.f	Average slope
Pionino	0–4	4.1	−0.56(18)
Partons $m_S=0$	0–4	1.9	−0.26(13)
Partons $m_S=0.22$	0–4	0.92	−0.23(13)
Pionino	0–3	8.3	−0.82(9)
Partons $m_S=0$	0–3	3.7	−0.39(13)
Partons $m_S=0.22$	0–3	2.2	−0.36(13)

a lesser improvement of the partonic data as compared to the hadronic ones as conjectured just above.

The slopes given in Table III are the averages over our set of momenta $\vec{q}$ (excluding the momentum corresponding to the white circle). We have kept the mass of the scalar parton between 0 and half the mass of the scalar-scalar bound state (see Table II). The resulting slopes do not depend significantly on the latter mass. It can also be seen that the slopes are quite similar for time slices [0,3] and [0,4].

B. Comparing three-point functions at $t=0$

Equation (18) predicts two main features of the partonic behavior: (i) the exponential time evolution; (ii) the following amplitude at $t=0$

$$F^0(\vec{p},\vec{q};t=0)\propto\frac{\Phi_\pi(u=1/2)}{2E_S(u=1/2)}. \tag{27}$$

The beginning of this section was devoted to the time evolution. Let us now focus on the amplitude (27).

The plot in Fig. 6 shows for our set of momenta $\vec{q}$ the product $E_S(1/2)F^0(\vec{p},\vec{q};0)$ which is expected to be constant from Eq. (27). E_S is computed from Eq. (13) with a massless scalar parton. The plotted ratio is indeed strikingly constant: the χ^2/d.o.f. for the fit to a constant ratio is 0.22. This expected constancy of a large set of numbers, which are significantly different from zero, yields amazing support to a partonic interpretation of these data. We cannot figure out any other explanation for this feature. Indeed, one might fear that the observed constancy of $E_S(1/2)F^0(\vec{p},\vec{q};0)$ is simply due to some contact term producing a $\vec{q}$ independent of $F^0(\vec{p},\vec{q};0)$ combined with a small dependence of $E_S(1/2)$ on $\vec{q}$. To consider this we have tried a fit with $F^0(\vec{p},\vec{q};0)$ = constant, which gives χ^2/d.o.f.=0.72, larger than the previously found 0.22, although still smaller than 1. We would thus rather believe, in agreement with the partonic interpretation, that the small variation of $F^0(\vec{p},\vec{q};0)$ is a consequence of the constancy of $E_S(1/2)F^0(\vec{p},\vec{q};0)$ and a small variation of $E_S(1/2)$. As a check, we have tested the constancy of $F^0(\vec{p},\vec{q};0)$ for $p=2\pi/L(1,0,0)$, which is not expected to follow Eq. (27) while contact terms have no reason to be absent.[15] We find χ^2/d.o.f.=2.7, which further supports the partonic interpretation of the constancy $E_S(1/2)F^0(\vec{p},\vec{q};0)$ for $p=2\pi/L(2,0,0)$.

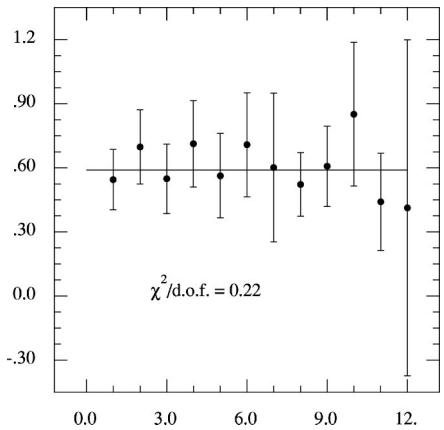

FIG. 6. Values of $E_S(1/2)F^0(\vec{p},\vec{q};0)$ normalized as Fig. 3 for $\vec{p}=(4\pi/L,0,0)$ and our full set of $\vec{q}$ (labeled from 1–12 on the horizontal axis). The data show the expected constancy around the average represented by the horizontal line.

VI. DISCUSSION AND CONCLUSION

We have performed the first tentative application of a new proposal [14] to compute the pion LCWF. This proposal was to compute the pion to vacuum matrix element of a nonlocal operator, namely the propagator of a scalar particle which has the color quantum numbers of a quark. For convenience, we call it a ''squark.'' This resulting matrix element is gauge invariant. To exhibit the partonic structure of the pion a large momentum $\vec{q}$ is added to the scalar propagator.

We have shown that, provided the pion has a large enough momentum $\vec{p}$, provided that the squark has a large enough energy, and provided the propagation time of the scalar object is short enough (end of Sec. II A), the above-mentioned matrix element is dominated by a contribution from the pion LCWF. A measure of this matrix element can then provide information on the LCWF.

A necessary first step is the computation of the two-point Green functions of quark (squark)-quark (squark) bound states. The new states, which contain at least one squark, show a behavior quite similar to standard hadrons, they show nice exponential time dependence (Fig. 1), they verify Einstein spectral law (Fig. 2), and the masses decrease with increasing κ_S, i.e., decreasing squark bare mass.

We have then analyzed the three-point Green functions for a large set of pion momenta $\vec{p}$ and transfers $\vec{q}$. The scalar parton has a momentum $u\vec{p}+\vec{q}$, where $u\in[0,1]$ is the fraction of pion momentum carried by the active quark. The discretization due to the finite volume implies a discretization of the fraction u. In our set, only the momentum $\vec{p}$

[15]We did not check the constancy of $E_S(1/2)F^0(\vec{p},\vec{q};0)$ in this case since $u=1/2$ is forbidden in the case $p=2\pi/L(1,0,0)$.

$=(2\pi/L)(2,0,0)$ allows for $u \neq 0,1$ (where the LCWF vanishes), namely $u=1/2$.

We focused the analysis on small times ($t \in [0,3-4]$) according to the formulas Eqs. (23) and (24) which express, respectively, the hypothesis of a partonic behavior of the squark and the spectator quark during this small time interval or, on the contrary, the hypothesis of a precocious confinement of the squark and the spectator quark into a hadronic-like bound state. The correct hypothesis should show up as a plateau in time.

Our data clearly favor the partonic behavior at small time: the observed rapid drop of the Green function is expected from a partonic picture, while a hadronic picture predicts a slower decrease. The analysis is however made delicate due to an observed vanishing of the Green function around $t=3-4$ which might be due to a destructive interference. The resulting analysis domain is very short and close to zero. This might induce the objection that we cannot disentangle our signals from lattice artifacts such as contact terms, etc.

Nevertheless, a second series of tests has confirmed our feeling that a real partonic signal shows up: all the Green functions at $t=0$ for our set of values of $\vec{q}$ verify the prediction, Eq. (27), of the partonic model (up to one unknown constant) in an amazing manner. It is difficult to figure out how a lattice artifact could mimic this behavior for so many data.

This work focused mainly on testing the viability of this program. We believe that the answer is positive. The fact that we could argue rather firmly that we see a partonic signal, obtained on a small lattice, with a rather large lattice spacing, and ''large'' momenta which are indeed not so large is encouraging.

In order to progress we first need to settle the question of possible lattice artifacts. To that aim, it would be necessary to change the lattice parameters and mainly a and to run a larger set of momenta. This would furthermore allow us to reach values of u other than 1/2 and provide an idea about the shape of the LCWF. This program implies the use of a larger volume, which would also hopefully reduce the noise of large momenta Green functions.

A recent work by Dalley based on a Hamiltonian formulation of QCD on a lattice [15] presents an interesting analysis of the LCWF. This new method is very promising although it presents some difficulties as stated by the author. It is of course too early to perform a detailed comparison of the Lagrangian formulation used here and also a Hamiltonian. Both need to be followed.

ACKNOWLEDGMENTS

We are specially grateful to Guido Martinelli and Damir Becirevic for the discussions that initiated this work. We thank Gregori Korchemsky and Claude Roiesnel for very instructive discussions. J. R-Q is indebted to Spanish Fundación Ramón Areces for financial support. These calculations were performed on the QUADRICS QH1 located in the Center de Resources Informatiques (Paris-sud, Orsay) and purchased thanks to a funding from the Ministère de l'Education Nationale and the CNRS. This work is supported in part by European Union Human Potential Program under Contract No. HPRN-CT-2000-00145 Hadrons Lattice QCD. Laboratoire de Physique Théorique is Unité Mixte de Recherche du CNRS-UMR 8627.

[1] S. J. Brodsky, Y. Frishman, G. P. Lepage, and C. Sachrajda, Phys. Lett. **91B**, 239 (1980); S. J. Brodsky, Y. Frishman, and G. P. Lepage, *ibid.* **167B**, 347 (1986); S. J. Brodsky and G. Peter Lepage, in *Pertubative Quantum Chromodynamics*, edited by A. H. Mueller (World Scientific, Singapore, 1989).

[2] S. J. Brodsky, hep-ph/9908456.

[3] S. J. Brodsky and G. R. Farrar, Phys. Rev. Lett. **31**, 1153 (1973).

[4] A. V. Efremov and A. V. Radyushkin, Theor. Math. Phys. **42**, 97 (1980).

[5] G. Bertsch, S. J. Brodsky, A. S. Goldhaber, and J. Gunion, Phys. Rev. Lett. **47**, 297 (1981).

[6] V. L. Chernyak and A. R. Zhitnitsky, Phys. Rep. **112**, 173 (1984).

[7] V. M. Braun and I. E. Filyanov, Z. Phys. C **44**, 157 (1998).

[8] G. Sterman and P. Stoler, Annu. Rev. Nucl. Part. Sci. **43**, 193 (1997).

[9] CLEO Collaboration, J. Gronberg *et al.*, Phys. Rev. D **57**, 33 (1998).

[10] P. Kroll and M. Raulfs, Phys. Lett. B **387**, 848 (1996); I. V. Musatov and A. V. Radyushkin, Phys. Rev. D **56**, 2713 (1997); A. Schmedding and O. Yakovlev, *ibid.* **62**, 116002 (2000); V. M. Braun, A. Khodjamirian, and M. Maul, *ibid.* **61**, 073004 (2000).

[11] Fermilab E791 Collaboration, E. M. Aitala *et al.*, Phys. Rev. Lett. **86**, 4768 (2001).

[12] V. M. Braun *et al.*, Phys. Lett. B **509**, 43 (2001); V. Chernyak, hep-ph/0103295.

[13] G. Martinelli and C. T. Sachrajda, Phys. Lett. B **190**, 151 (1987); Nucl. Phys. **B316**, 305 (1989).

[14] U. Aglieti, M. Ciuchini, G. Corbò, E. Franco, G. Martinelli, and L. Silvestrini, Phys. Lett. B **441**, 371 (1998).

[15] S. Dalley, Phys. Rev. D **64**, 036006 (2001).